

Molecular Docking and Molecular Dynamic Simulation of Potential Inhibitors of Integrase from Human Immunodeficiency Virus 1 (HIV-1) Using Phytochemicals

Vikas Jha^{1,*}, Navdeep Kaur¹, Kabir Thakur¹, Vrushali Dhamapurkar¹, Prakruti Kapadia¹, Shraddha Tiwari², Aparna Sahu², Divya Nikumb¹, Abhishek Kumar¹, Shruti Narvekar¹

¹National Facility for Biopharmaceuticals, Guru Nanak Khalsa College of Arts, Science & Commerce, Mumbai, India

²Department of Biotechnology, B. K. Birla College, Kalyan, India

Email address:

vikasjjha7@gmail.com (V. Jha)

*Corresponding author

To cite this article:

Vikas Jha, Navdeep Kaur, Kabir Thakur, Vrushali Dhamapurkar, Prakruti Kapadia, Shraddha Tiwari, Aparna Sahu, Divya Nikumb, Abhishek Kumar, Shruti Narvekar. Molecular Docking and Molecular Dynamic Simulation of Potential Inhibitors of Integrase from Human Immunodeficiency Virus 1 (HIV-1) Using Phytochemicals. *Computational Biology and Bioinformatics*. Vol. 10, No. 1, 2022, pp. 34-48. doi: 10.11648/j.cbb.20221001.16

Received: May 30, 2022; Accepted: June 22, 2022; Published: June 30, 2022

Abstract: Background: In tremendously effective antiretroviral therapy for Human Immunodeficiency Virus 1 (HIV1) infections, integrase inhibitors are essential drugs. Resistance resulting from mutations, on the other hand, poses a threat to the medication's long-term efficacy in HIV-1 infected people. Purpose: The current study utilized in silico techniques, we searched for phytochemicals or compounds that can inhibit the activity of the integrase enzyme. Material & Methods: Compounds were collected from databases, and potential candidates were screened using pharmacokinetics and structure-based virtual screening methodologies. The compounds were docked, and the binding affinity was evaluated to set the cut-off value for selecting compounds. When compared to standard drugs, some compounds had a higher binding affinity. Molecular dynamics simulation was then used to gain insight into the stability of the complexes, revealing two lead compounds, Withaferin and Isatin, indicating that these compounds have potency for drug development. These compounds were further investigated for their toxicity, indicating that Isatin was safe among the two. Conclusion: Thus, the study showcased that Isatin is a suitable drug candidate, and we hope that the findings of this study will be useful in the development of an antiviral drug against integrase enzyme.

Keywords: Human Immunodeficiency Virus 1 (HIV1), Integrase, Molecular Docking, Molecular Dynamic Simulation

1. Introduction

In 1983, the HIV virus was isolated and recognized for the first time, and since then about 75.7 million people have been infected with HIV and 32.7 million have died due to AIDS-related illnesses (<https://www.avert.org/global-hiv-and-aids-statistics>). The virus is believed to have spread to humans from non-human primates in Africa via cross-species transmission [1]. Multiple transmissions have occurred since then, but the effects have been wildly disparate; some have resulted in global pandemics, while the others appear to have caused little or no human spread. The HIV virus is

categorized into types, groups, subtypes, circulating recombinants forms (CRFs), and unique recombinants forms (URFs) using phylogenetic analysis of the isolates taken from patients living across diverse geographic regions [2]. HIV-1 strains are divided into three lineages: group M, group N, and group O. These lineages appear to be the result of a separate transmission from central African chimps. HIV-2 has originated from the sooty mangabey monkeys in West Africa. The main HIV pandemic is caused by HIV-1 group M strains, which is thought to have evolved into genetic

subtypes after being introduced to humans. HIV-1 groups N and O are extremely rare, occurring only in Cameroon in Central Africa [3]. The prevalence and the spread of HIV-2 has decreased as observed since the last 30 years [4]. Today, HIV/AIDS is one of the most serious public health threats.

HIV encodes three essential viral enzymes: viral protease, reverse transcriptase, and integrase. (Figure 1) The drugs for the AIDS treatment include protease inhibitors, reverse transcriptase inhibitors, co-receptor inhibitor, fusion inhibitors, and the newly added integrase inhibitors [5-7]. Inhibitors of the viral protease enzyme and non-nucleoside and nucleoside inhibitors of the reverse transcriptase are used for the treatment of infection in combinations known as HAART (highly active antiretroviral therapy). HAART has undeniably had a positive impact on treatment of HIV infection, but resistance to these

classes of inhibitors has diminished their efficacy, driving the search for new inhibitors [8].

Integrase is the enzyme responsible for integrating the viral DNA into the host chromosome [9]. Integration begins by cleaving the viral DNA 3'ends, which then attacks the host DNA (tDNA), which is later followed by DNA repair. The 3' processing and DNA integration occur in an active site that requires the presence of two Mg^{2+} cofactors following 3' processing. This active site becomes a target of the drug family integrase strand transfer inhibitor (INSTI) [10]. In spite of intensive research on HIV integrase, only four FDA-approved drugs currently exist against the integrase enzyme; 'Raltegravir, Elvitegravir, Cabotegravir and Dolutegravir' ([http:// www.fda.gov](http://www.fda.gov)), which are administered along with other antiretroviral medications.

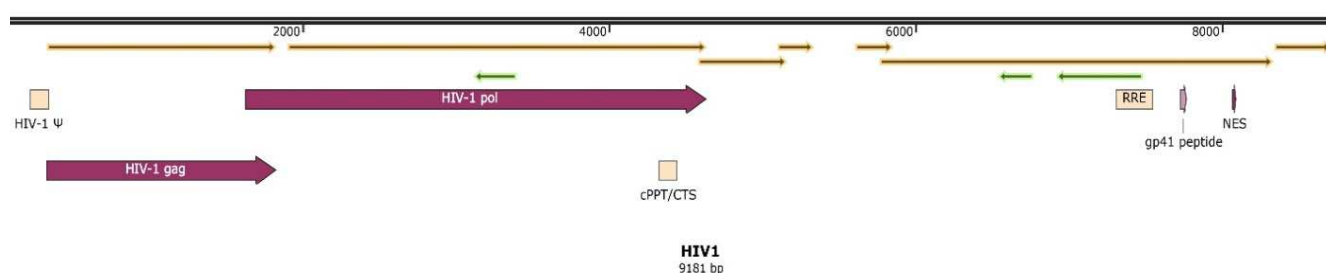


Figure 1. Proteins distributed in the HIV-1 genome. Figure created using NC_001802.1.

They block the strand transfer reaction; thus, they are also referred as Integrase strand transfer inhibitors (INSTI) [5-7]. These drugs are generally well tolerated, although side-effect profiles differ between drugs. People who experience adverse effects with one INSTI may tolerate an alternative drug in this class; however, switching from one INSTI to another may result in new side effects [11]. Integrase is one of the most crucial enzymes required for the viral replication, making it a reasonable target for antiviral agents and thus recent research has focused on new integrase inhibitors including those targeting non-catalytic sites of HIV integrase [8, 12].

The development of novel molecular scaffolds with high binding affinity and selectivity for the target, as well as a suitable pharmacokinetic profile is one of the key goals in drug discovery. To identify new inhibitors, virtual screening protocols have been proposed such as docking, pharmacophore mapping, and shape-based screening (SBS) [13]. Molecular docking can be used for screening of the potential molecules acting against the HIV integrase from a large dataset and based on the docking studies, the identified potent molecules can be subjected to pharmacokinetics and drug-likeness studies. The goal of molecular docking is to find realistic binding geometries for a proposed ligand with a known target site; this is carried out by characterizing the binding site, correctly aligning the ligand in the binding site, and estimating the strength of the ligand- receptor complex interaction [14]. The potent chemical molecules identified through molecular docking are more likely to progress to the next stage of the drug development process. Thus, in vitro and in silico approaches are now widely used to investigate

the pharmacokinetics of new chemical entities and molecular modelling have been most widely used tool to optimize leads in drug development [15].

Most drugs in the market nowadays are either derived from natural sources or are semi- synthetic in origin. Some analogues of the natural compounds for some new targets in HIV-1 may be developed as the new anti-HIV drugs. Thus, natural molecules could be a promising alternative for developing a novel drug. The use of phytochemicals to be explored as anti-HIV agents could be another viable option [16]. In consideration of these studies, we have performed a molecular docking study of ligands against HIV integrase. The further information from this study would be helpful to explore a new compound, which could be very useful for further refined and lead optimization process in the development of HIV integrase antiretroviral drugs.

2. Material and Methods

2.1. Protein Retrieval

This analysis was based on the 3D structure of HIV-1 Integrase Protein as it plays an essential role in viral replication and integration of viral genome into the host [17]. The 3-D structure of the Integrase Protein was obtained from the RCSB PDB data repository in PDB format. The PDB id of the selected structure is 6JCF. (<https://www.rcsb.org/structure/6JCF>) [18]. The 3D structure of the Integrase protein can be observed in (Figure 2).

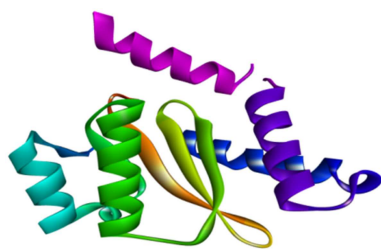


Figure 2. 3-Dimensional structure of the Integrase Protein of HIV-1 Virus.

2.2. Ligand Retrieval

In this study, 2099 ligands were selected, out of which 99 were antiviral drugs derived from Dr Duke's Drug Bank database [19] and 2000 ligands were phytochemicals retrieved from Indian Medicinal Plants, Phytochemistry and Therapeutics (IMPPAT) database [20]. The 3-D SDF files of these compounds were collected from the PubChem database. (<https://pubchem.ncbi.nlm.nih.gov/>) [21].

2.3. ADME Analysis

Swiss-ADME (<http://www.swissadme.ch/>) [22] webserver was utilized for screening purposes on the basis of Lipinski's rule of five. The ADME analysis provides prediction of the in vivo behavior of a ligand thus indicating its potential to be a viable drug candidate. In order to qualify as a ligand, a compound should have a molecular mass of less than 500 Daltons, an octanol-water partition coefficient (log P) that does not exceed 5, less than 10 H-bond donors, no more than 5 hydrogen bond donors (the total number of Nitrogen-Hydrogen and Oxygen-Hydrogen bonds) [22, 23].

2.4. Bioavailability Radar

The bioavailability radar of the shortlisted drugs candidates following Lipinski's rules were retrieved using the Swiss-ADME which was centered on physicochemical indices suitable for oral consumption such as LIPO, Lipophilicity: $-0.7 < \text{XLOGP3} < +5$; SIZE, Molecular size: $150 \text{ g/mol} < \text{mol. wt.} < 500 \text{ g/mol}$; POLAR, Polarity: $20 \text{ \AA}^2 < \text{TPSA} < 130 \text{ \AA}^2$; INSOLU, Insolubility: $0 < \text{Log S (ESOL)} < 6$; INSATU, Instauration: $0.25 < \text{Fraction Csp3} < 1$; FLEX, Flexibility: $0 < \text{Number of rotatable bonds} < 9$. The colored zone within the radar is the physicochemical space which indicates oral bioavailability. Any deviation from these parameters on a large scale suggests that the ligand cannot be orally consumed [22].

2.5. Protein and Ligand Preparation

Protein: The 3D Structure of integrase protein was selected for molecular docking analysis using UCSF Chimera 1.15 tool [24]. The water molecules were removed, Kollman charges and polar hydrogen atoms were added to the protein molecule, and finally the charged protein molecule was saved in PDB format.

Ligand: Bioactive compounds which satisfied the Lipinski's rule of five were chosen as ligands, and their structures were obtained from PubChem databank in SDF

format. PyRx Virtual Screening Tool was utilized to generate structure variations, to optimize and minimize energy of the ligands [25].

2.6. Molecular Docking

The molecules following Lipinski's rule of five were subjected to molecular docking. The selected ligand structures were docked with the Integrase protein of HIV-1 virus using Auto Dock Vina [26]. The Auto Dock Vina software carries out the prediction of bound conformation based on free binding energies, which was calculated on the basis of the empirical force field. The docking analysis was performed using the Auto Dock Vina via docking protocol PyRx Virtual Screening Tool. This evaluation helped in narrowing down the potential ligands exhibiting high binding affinity with the protein as probable inhibitors.

2.7. Analyzing and Output Visualization

The docking pose having the lowest free binding energy to the corresponding protein was analyzed using Biovia Discovery Studio Visualizer [27]. The ligands showing ideal binding energy (above $7.5 \text{ kcal}\cdot\text{mol}^{-1}$) were selected and analyzed via 2- and 3-dimensional protein-ligand complexes, and based on their intermolecular interactions, such as hydrogen bonding, hydrophobic interactions, Van-der Waal forces, alkyl bonds, pi-alkyl bonds, sigma bonds, pi-sigma bonds, pi-cation bonds, pi-anion bonds, and pi-pi T-shaped bonds.

2.8. Molecular Dynamics Simulations

The molecules exhibiting higher binding affinity were subjected to WEBGRO, which is a highly autonomous online platform, for performing molecular dynamics simulation to study the interactions established by these ligands with their target protein. GROMACS simulation package is utilized for performing fully solvated molecular dynamics simulations [28]. Molecular dynamics simulations confirm and calculate the stability, fold, and interactions of the docked proteins. The simulations were performed at 100 ns. The MD simulations parameters were kept as follows Forcefield: GROMOS96 43a1, Water model: SPC, Box Type: Triclinic, Salt Type: NaCl, Neutralization with 0.15M salt; Energy Minimization parameters- Integrator: Steepest Descent, Steps: 5000, Equilibration, and MD run Parameters-Equilibration Type: VT/NPT, Temperature (K): 300, Pressure (bar): 1.0, MD integrator: Leap-frog, Simulation time (ns): 100 (max allowed 100nsec), Approximate number of frames per simulation: 1000, Webgro: time 100 ns. The conformational changes seen in the structural level integrity of docked complexes were analysed using root mean square deviation (RMSD).

2.9. Toxicity Prediction

Toxicity prediction was performed for the drugs showing zero violations of the Lipinski's rule to evaluate the safety of drugs for human consumption. The absorption, distribution, metabolism, excretion, and toxicological characteristics of the

compounds employed in this study were calculated (ADMET). ProTox-II, a virtual lab for predicting small molecule's toxicity, and ADMET 2.0 were used for the analysis. The drugs were uploaded to the server which gave results exhibiting the toxicity prediction. ProTox II tool [29] was used to calculate the toxicity profiles, toxicity class, and LD50 values of the shortlisted phytochemicals. Based on the LD50 value of 3700 dataset compounds, it determines the toxicity of the compound and categorizes the query drug into six broad groups, with Class I being extremely toxic and Class VI being safest. This server also specifies the prescribed mg/kg value of the medication for consumption. ADMET 2.0, an integrated online platform for accurate and comprehensive predictions of ADMET properties, [30] was also used to determine certain toxicity parameters which are required for a molecule to qualify as an ideal drug. The parameters evaluated through ADMET includes Herg Blockers, H-ht, DiliAmes toxicity, Eye irritation, Rat oral acute toxicity, Fdamdd, Skin sensitization, Carcinogenicity, Eye corrosion, Respiratory toxicity, and Environmental toxicity.

3. Result and Discussion

For decades, finding a cure for HIV has been difficult. To stop the virus from spreading in the host, numerous compounds have been explored against specific components of the virus. The concept of using a known phytochemical to develop cure for the disease is intriguing [31]. The enzymes encoded by the virus are viral protease, reverse transcriptase, and integrase. HIV integrase is a rational target for treating HIV infection and preventing AIDS. The HIV integrase (IN) enzyme is a 32-kDa protein encoded by the *pol* gene of the virus [32]. The 3D structure of the HIV-1 Integrase Protein, which is required for viral replication and integration of the viral DNA into the host, was retrieved in PDB format from the RCSB PDB data repository. In this study, we have investigated the binding of different inhibitors to the enzyme using computational docking approaches.

A total of 2099 ligands were chosen, Out of those 99 Ligands were selected from Dr Duke's Drug Bank database and the remaining 2000 were selected from the Indian Medicinal Plants, Phytochemistry and Therapeutics (IMPPAT) database [19, 20]. The compounds chosen were flavonoids, organic compounds, alkaloids, polyphenols, terpenoids, carboxylic acids, steroids, quinones, carbohydrates, benzene and derivatives, and lipids and fatty acids.

3.1. Evaluation of Pharmacokinetic and Pharmacological Properties

Lipinski's rule of five was used to determine a compound's drug likeness. Lipinski's rule of five, which is based on lipophilicity, molecular weight, and hydrogen donor-acceptor bonds predicts the absorption and the penetration of drug. The absorption of the drug into the system, distribution, metabolism, and then the excretion of the drug is based on this rule [32]. For enhanced selectivity and drug-like physicochemical qualities, the properties of the molecule

must be in accordance with the rule of five. The molecule should have H bond acceptors < 10, H bond donors < 5, molecular weight of < 500 and Log P < 5, indicating high lipophilicity [33]. The interaction between the drug and the membrane is affected when these rules are violated. Smaller lipophilic molecules have a higher permeability, furthermore, when the drug molecule has a positive charge, passive diffusion is preferred since it has a better interaction with the cell membrane [34]. Lipinski's rule of five was used to determine the drug-likeness of 2099 bioactive compounds in this study. As observed in (Figure 3), 15.86% of the compounds were flavonoids, 14.48% were organic compounds, 14.15% of the compounds were not classified into any group, whereas the remaining compounds included alkaloids, polyphenols, terpenoids, carboxylic acids, steroids, quinones, carbohydrates, benzene and derivatives, and lipids and fatty acids which accounted for 6.86, 3.67, 13.24, 5.96, 5.81, 1.24, 6.38, 7.38, and 4.95%, respectively. As shown in (Figure 4), 41.50% of the compounds followed Lipinski's rule of five, while 24.73, 15.01, 11.62, and 7.15% disobeyed one, two, three, and four rules, respectively. Compounds that violated one or more of Lipinski's rules were excluded from the study, and only 871 compounds were further investigated.

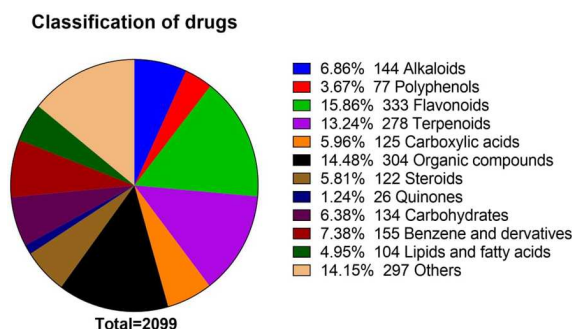


Figure 3. Classification of the drugs.

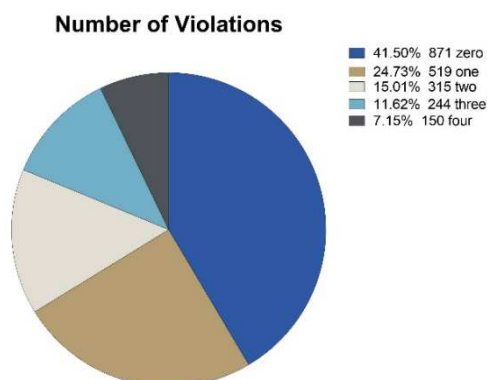


Figure 4. Distribution of drugs based on Lipinski's rule of five.

3.2. Bioavailability Radar and Toxicity Prediction

Following the ADME analysis, molecular docking, and molecular dynamic stimulations, all the 871 compounds were further investigated for their toxicity profile. An expository tool- Bioavailability radar- was used to elucidate the drug-likeness of the compound. To detect drug-likeness, the tool

predicts the bioavailability radar based on six physicochemical properties: size, solubility, lipophilicity, flexibility, polarity, and saturation [35]. Because of its convenience of administration, cost-effectiveness, less sterility limitations, and flexibility in design of dosage, oral ingestion is convenient and widely used mode of drug delivery in the patients. As a result, many drug manufacturers are more likely to produce bioequivalent oral drug formulations [36]. However, around forty percent of new drug compounds have poor water solubility, thus making oral administration difficult due to high intra- and inter-subject variability, low bioavailability, and a lack of dose design. When it comes to the production or research on a new oral drug, low aqueous solvency is a major concern. For these oral drugs, limited water dissolvability and high lipophilicity limit the therapeutic effect. It is recommended to increase the bioavailability and decreasing interpatient changeability in plasma level concentrations [37]. A drug that has low aqueous solubility will also have low saturation solubility, thus its bioavailability will be low. To interact with the lipid membrane, a medication should have sufficient lipophilicity. A deviation from these parameters shows that the ligands are not orally bioavailable [38, 39]. All the 871 compounds studied were found to be orally bioavailable. Safety of the drug, which includes a variety of toxicities and side effects, is

still the most pressing concern during drug development. To avoid significant financial losses later in the process of drug development, computational methods and approaches can be used which have proven to be more advantageous over in vitro and in vivo studies [40]. The shortlisted molecules were subjected to additional testing using the PROTOX -II webtool for toxicity analysis. The parameters used for the evaluation of the compounds were: Toxicity class (Oral toxicity), Predicted LD50, Hepatotoxicity, Carcinogenicity, Immunotoxicity, Mutagenicity, and Cytotoxicity.

Considering the bioavailability radars (Figure 5) of the best ligands and the toxicity profile, (Table 1) it can be deduced that Isatin is a potential candidate for drug development, and it can be used for the treatment of HIV infection. In comparison to other ligands, it has a high LD50 value (1000 mg/kg) and shows the maximum number of hydrogen bonds with the receptor. However, it possesses carcinogenicity, which makes it unsuitable for oral consumption. Further analysis needs to be carried out to reduce its carcinogenicity for making it a potential lead molecule for formulation development. Withaferin, Cladospirone bisepoxide, and 4,8-Dihydroxysesamin are bioavailable, and they also show the presence of hydrogen bonds. Thus, they can be used to treat HIV infection, but the dosage of those molecules must be calculated because they possess toxicity and carcinogenicity.

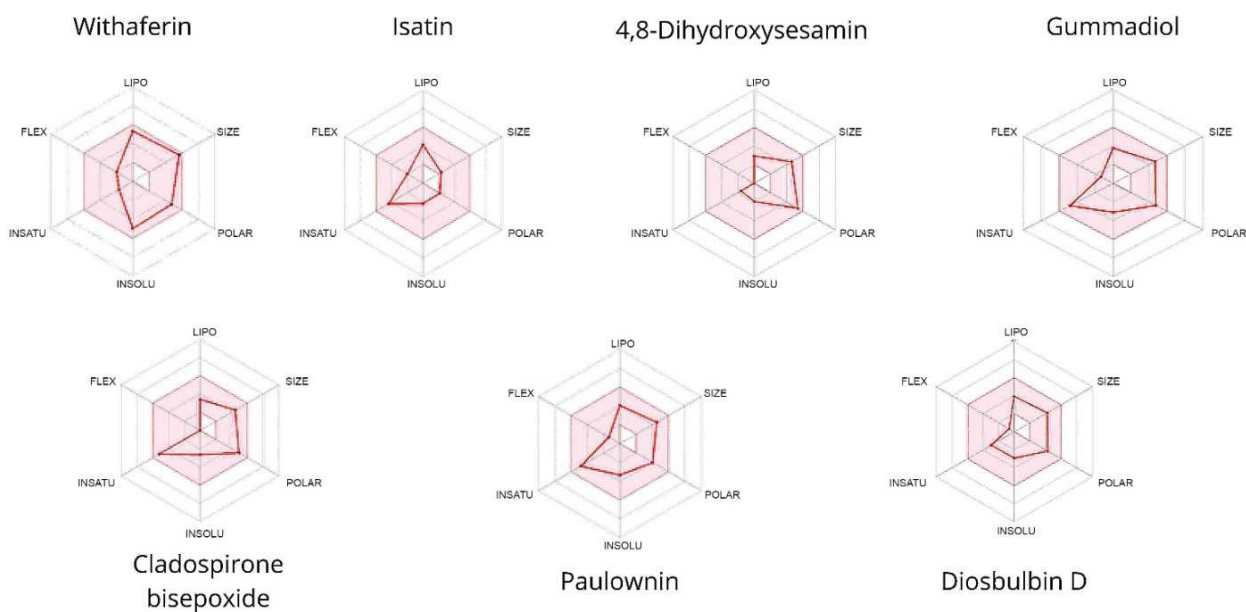


Figure 5. Bioavailability Radar diagram of the best ligands.

Table 1. Toxicity prediction of the best ligands.

Ligands	Class	LD 50 (mg/kg)	Hepato-toxicity	Carcino-genicity	Immuno-toxicity	Muta-genicity	Cyto-toxicity	Conventional hydrogen bonds
Withaferin	3	300mg/kg	Inactive	Inactive	Active	Inactive	Active	4
Isatin	4	1000mg/kg	Inactive	Active	Inactive	Inactive	Inactive	4
Gummadiol	3	1500mg/kg	Inactive	Inactive	Active	Inactive	Inactive	-
Cladospirone bisepoxide	2	34mg/ kg	Inactive	Active	Inactive	Active	Inactive	3
Paulownin	3	1500mg/kg	Inactive	Inactive	Active	Inactive	Inactive	-
4,8-Dihydroxy-sesamin	3	1500mg/kg	Inactive	Active	Inactive	Inactive	Inactive	2
Diosbulbin D	3	280mg/kg	Inactive	Inactive	Active	Inactive	Inactive	-

3.3. Molecular Docking

Molecular docking is one of the most successful and common structure-based *in silico* strategy for predicting the interactions between molecules and their biological targets. It is usually performed by first predicting the molecular orientation of a ligand within a receptor, and then using a scoring function to estimate their complementarity [41, 42]. It selects the best protein-ligand pair based on their binding affinity and assists the drug developer in moving forward with testing the most promising drug candidate. The bioavailable ligands were used to perform molecular docking with the HIV integrase enzyme. (Table 2) shows the binding energy values for the top 7 ligands, their binding energies indicate that they have a good affinity for the target enzyme; integrase. Whereas (Table 3), shows the binding energy values of the drugs used for the treatment of HIV. As observed from the (Figure 6), the phytochemicals have same and, in some cases, even higher binding energies as compared to the drugs used in the treatment of HIV. The phytochemicals withaferin, isatin, gummadiol, and cladospirone bisepoxide have a higher affinity than the drugs used for the treatment currently, their binding energies are -8.3, -8, -7.7, and -7.7, respectively. The binding energies of the drugs dolutegravir, cabotegravir, elvitegravir, and raltegravir are -7.2, -7.6, -6.6, and -7.2, respectively. The phytochemicals with higher binding energies might have more hydroxyl groups, which generate hydrogen bonds with the target protein indicating that they have a favorable interaction with the target. Also, bonds such as alkyl and pi-alkyl promote the hydrophobic interaction of ligands in the receptor's binding pocket. The pi-sigma bond introduces stabilizing charges that allow the drug to intercalate into the receptor's binding sites. All negative atoms, such as chlorine atoms, are balanced by the pi-cation bond. These bonds play an important role in the structural binding and free energies of the ligands with their respective targets [38, 43]. Considering the best ligands, the binding affinity was in the range of -8.3 to -7.6 (Table 2 and Figure 6), suggesting that Withaferin (-8.3) is a better candidate as compared to the other ligands.

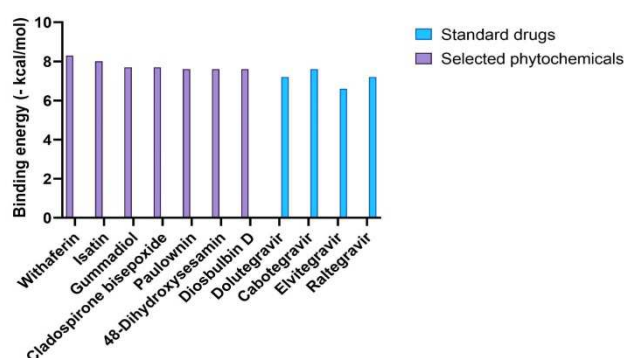


Figure 6. Comparative binding energy of the best ligands and the drugs currently employed for the treatment of HIV.

Table 2. Binding Energy of HIV integrase with top 7 phytochemicals as ligands.

Sr. No	Ligand	Binding Energy n(ΔG) (kcal/mol)
1	Withaferin	-8.3
2	Isatin	-8
3	Gummadiol	-7.7
4	Cladospirone bisepoxide	-7.7
5	Paulownin	-7.6
6	4,8-Dihydroxysesamin	-7.6
7	Diosbulbin D	-7.6

Table 3. Binding Energy of HIV integrase with drugs currently used for treatment.

Sr. No	Ligand	Binding Energy n(ΔG) (kcal/mol)
1	Dolutegravir	-7.2
2	Cabotegravir	-7.6
3	Elvitegravir	-6.6
4	Raltegravir	-7.2

3.4. Molecular Dynamics Simulations

The WEBGRO server was used to evaluate the stability of the top seven inhibitor-integrase complexes. Molecular dynamic simulation was performed to investigate the RMSD and RMSF values of the selected inhibitors. The Root Mean Square Deviation (RMSD) is the measure of the average distance between atoms of two superimposed molecules. It can be used to evaluate the stability of a given system. The Root Mean Square Fluctuation (RMSF) is a measure of atoms or group of atoms' displacements relative to a reference structure, averaged over the number of atoms present. It is used to evaluate the stability of a structure over the duration of simulations [44]. A high RMSF value indicates the protein structure's flexibility, the presence of loops, or the loose bonding between the molecules, whereas a low value indicates stability as well as the presence of secondary structures such as sheets and helices. The Solvent Accessible Surface Area (SASA) is the surface area of a protein-ligand complex that interacts directly with solvent molecules. The rise in the values indicates relative expansion, and lower values imply more stability. Hydrogen bonds are important in determining the specificity of ligand binding. They are regarded as an important parameter in drug designing because they play a role in drug metabolism, and absorption.

Withaferin has a binding energy of -8.3 kcal/mol. It has two types of bonds: the conventional hydrogen bond and the alkyl bond. LYS A-185, GLU A-198, ASN A-184 formed the conventional hydrogen bond. PHE 181, TYR 83, and VAL 201 of the A chain formed an alkyl bond with the ligand. (Figure 7) The RMSF plot (Figure 8a)) shows that the molecule has higher RMSF values indicating that the protein has loops or turns. The value of the radius of gyration (R_g) indicates the stability of the complex, which can be correlated to the compactness of the structure. (Figure 8b)) The solvent accessible surface area plot shows fluctuations during binding of the ligand. (Figure 8c)) A maximum of four hydrogen bonds can be seen between the receptor and

Withaferin. (Figure 8d)) The RMSD plot for the receptor in complexation with Withaferin (Figure 8e)) was observed, it showed equilibria between 25 to 70 ns and it was in the range

of 1.35 to 1.65 Å. This molecule can be further investigated for drug development due to the presence of hydrogen bonds and overall stability of the complex.

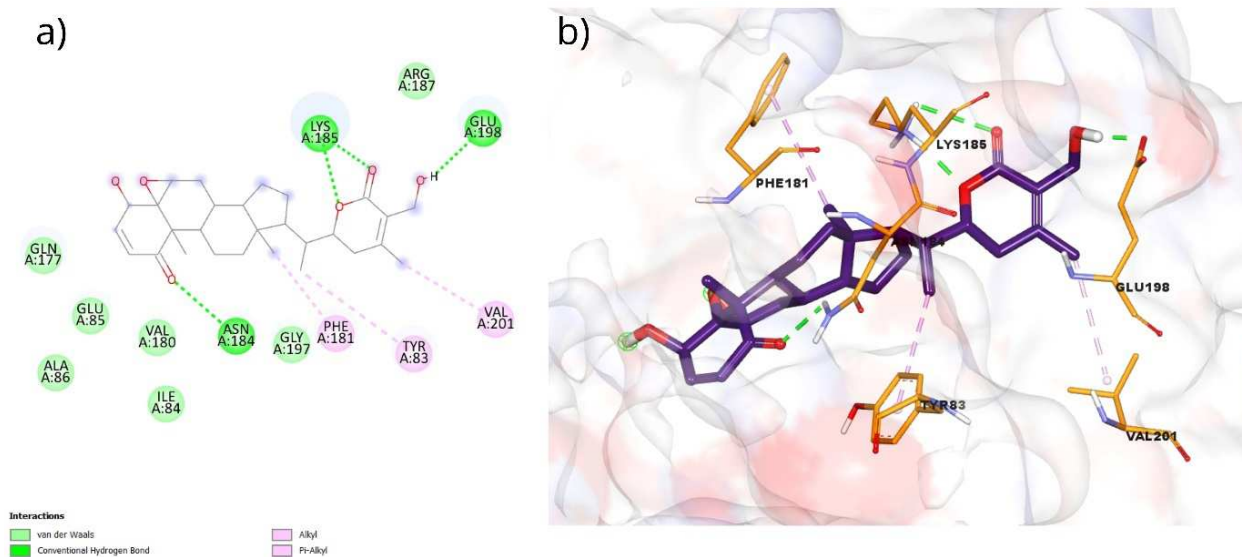


Figure 7. 2D interaction plot of Withaferin docked in the binding pockets of integrase enzyme. 3D representation showing the position of Withaferin within the cavity of integrase enzyme.

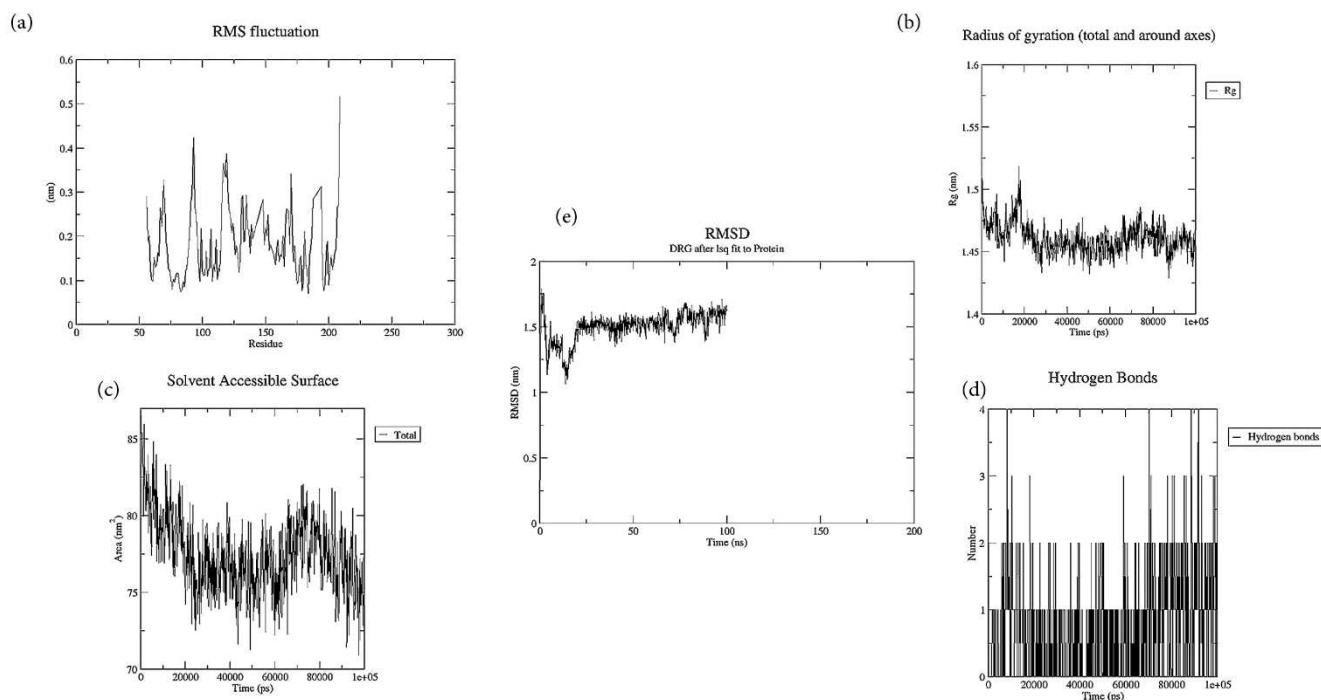


Figure 8. RMSF plot of the receptor-Withaferin complex. The Radius of Gyration plot of the receptor-Withaferin complex. The Solvent Accessible Surface area plot of the receptor-Withaferin complex. Hydrogen bonding pattern of the receptor-Withaferin complex. RMSD study plot of the receptor-Withaferin complex.

Isatin has binding energy -8 kcal/mol and displays altogether three types of interactions. LYS 188, LYS 186, and GLU 157 of the chain A displayed alkyl and pi-anion bonds, respectively. ARG 199, ALA 196, LYS 186 of the A chain formed conventional hydrogen bonds. (Figure 9) The RMSF plot (Figure 10a)) displays that the molecule has higher RMSF value, but the values are lower than Withaferin. The value of the radius of gyration (Rg) shows stability with

some fluctuations. (Figure 10b)) The solvent accessible surface plot shows slight fluctuations but has stability overall. (Figure 10c)) Four hydrogen bonds can be seen between the receptor and Isatin. (Figure 10d)) In the receptor-Isatin complex, the RMSD values (Figure 10 e)) were in the range $4.5 - 5.0$ Å with some fluctuations. The equilibration of the complex was observed between 25 to 100 ns. Isatin can be a promising candidate for drug development

and further studies can be carried out to elucidate the activity of the molecule.

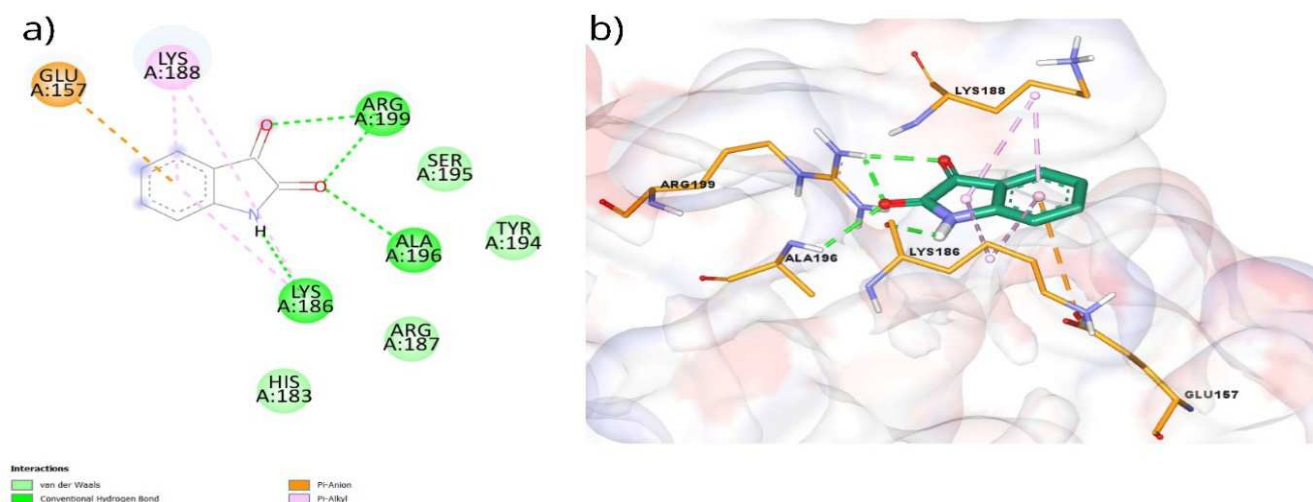


Figure 9. 2D interaction plot of Isatin docked in the binding pockets of integrase enzyme. 3D representation showing the position of Isatin within the cavity of integrase enzyme.

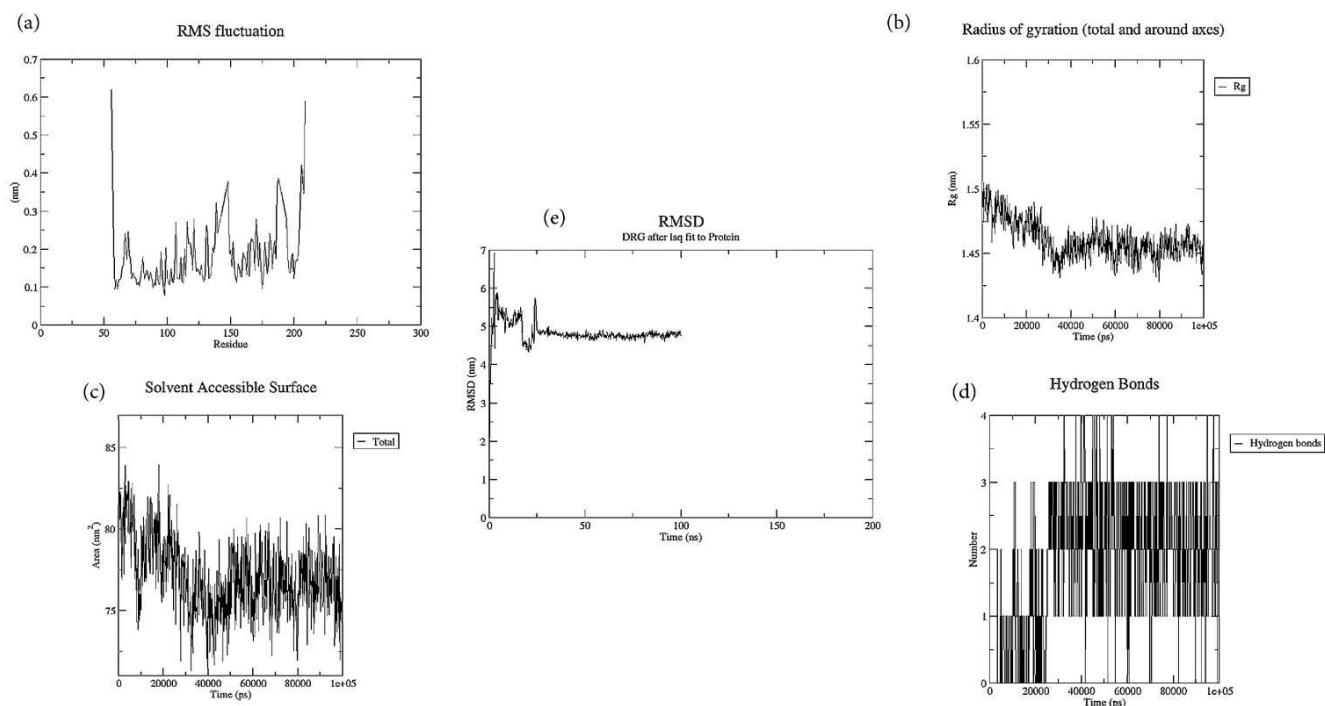


Figure 10. RMSF plot of the receptor-Isatin complex. The Radius of Gyration plot of the receptor-Isatin complex. The Solvent Accessible Surface area plot of the receptor-Isatin complex. Hydrogen bonding pattern of the receptor- Isatin complex. RMSD study plot of the receptor-Isatin complex.

The binding energy of Gummadiol is -7.7 kcal/mol. It displays different types of interactions, which includes carbon hydrogen bond, pi-alkyl bond and alkyl bond. LYS 127 of the A chain formed a carbon hydrogen bond. A chain residue CYS 130 forms pi-alkyl bond. A chain residues VAL 113, PHE 121, ILE 135, LYS 127, and LUS 136 interact with ligand by forming alkyl bonds. (Figure 11) The RMSF plot (Figure 12a)) shows that Gummadiol has higher RMSF values. The radius of gyration (Rg) plot shows fluctuations

and does not attain stability throughout the simulation. (Figure 12b)) The solvent accessible surface area plot displays significant fluctuations. (Figure 12c)) No hydrogen bonds were formed between the receptor and Gummadiol. (Figure 12d)) The receptor-Gummadiol complex showed RMSD (Figure 12e)) values in the range 0.75 – 2.90 Å with multiple fluctuations. The equilibration of the complex was observed between 10 – 45 ns.

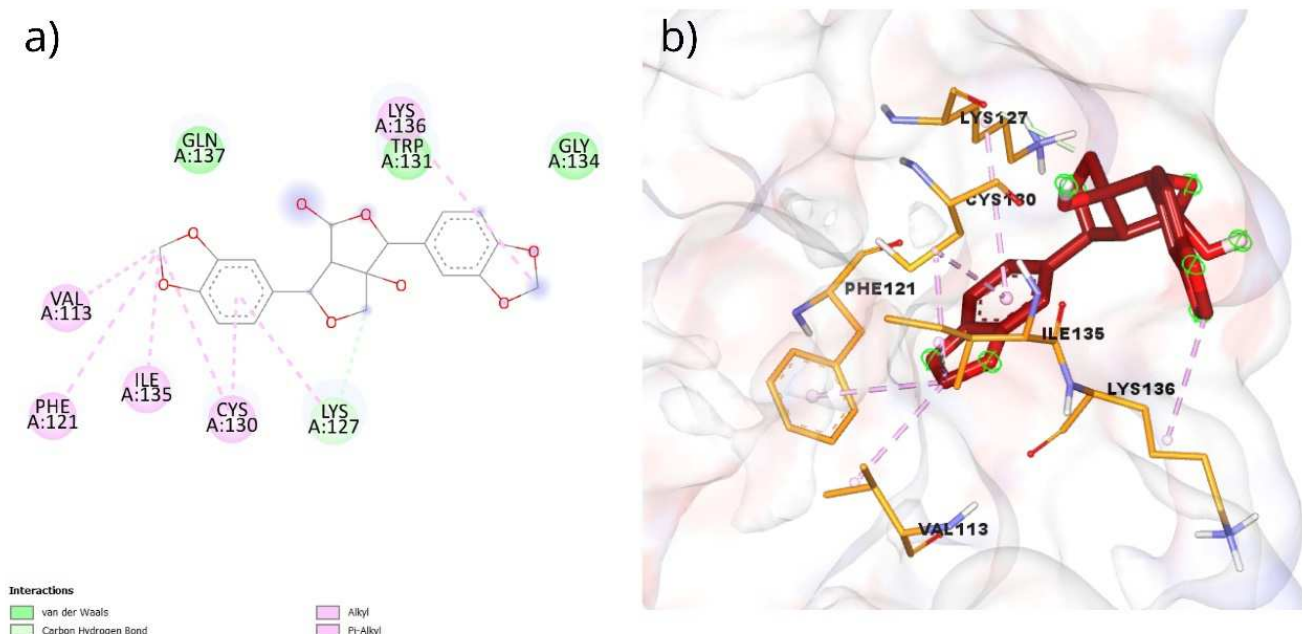


Figure 11. 2D interaction plot of Gummadiol docked in the binding pockets of integrase enzyme. 3D representation showing the position of Gummadiol within the cavity of integrase enzyme.

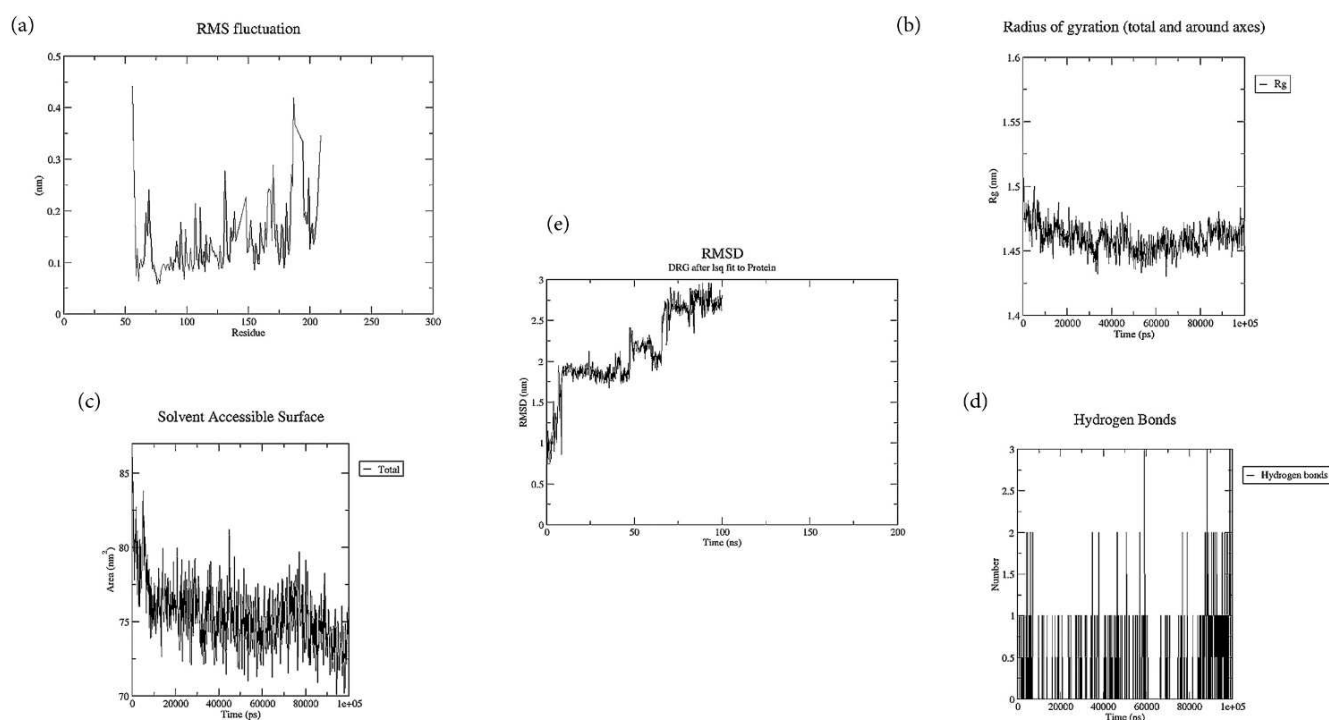


Figure 12. RMSF plot of the receptor-Gummadiol complex. The Radius of Gyration plot of the receptor-Gummadiol complex. The Solvent Accessible Surface area plot of the receptor-Gummadiol complex. Hydrogen bonding pattern of the receptor-Gummadiol complex. RMSD study plot of the receptor-Gummadiol complex.

Cladospirone bisepoxide has binding energy -7.7 kcal/mol and displays altogether two types of interactions. GLN 177 and ASN 184 of the chain A formed conventional hydrogen bonds. TYR 83 of the A chain formed pi-pi T-shaped bond. (Figure 13) The RMSF plot (Figure 14a)) shows that the molecule has higher RMSF value. The radius of gyration (Rg) plot shows considerate fluctuations. (Figure

14b)) The solvent accessible surface area plot also shows fluctuations throughout the simulation. (Figure 14c)) Cladospirone bisepoxide forms three hydrogen bonds with the receptor. (Figure 14d)) The RMSD plot for the receptor in complexation with Cladospirone bisepoxide (Figure 14e)) was observed, it showed equilibria between 10 to 60 ns, and it was in the range of 2.4 to 3.3 Å with some fluctuations.

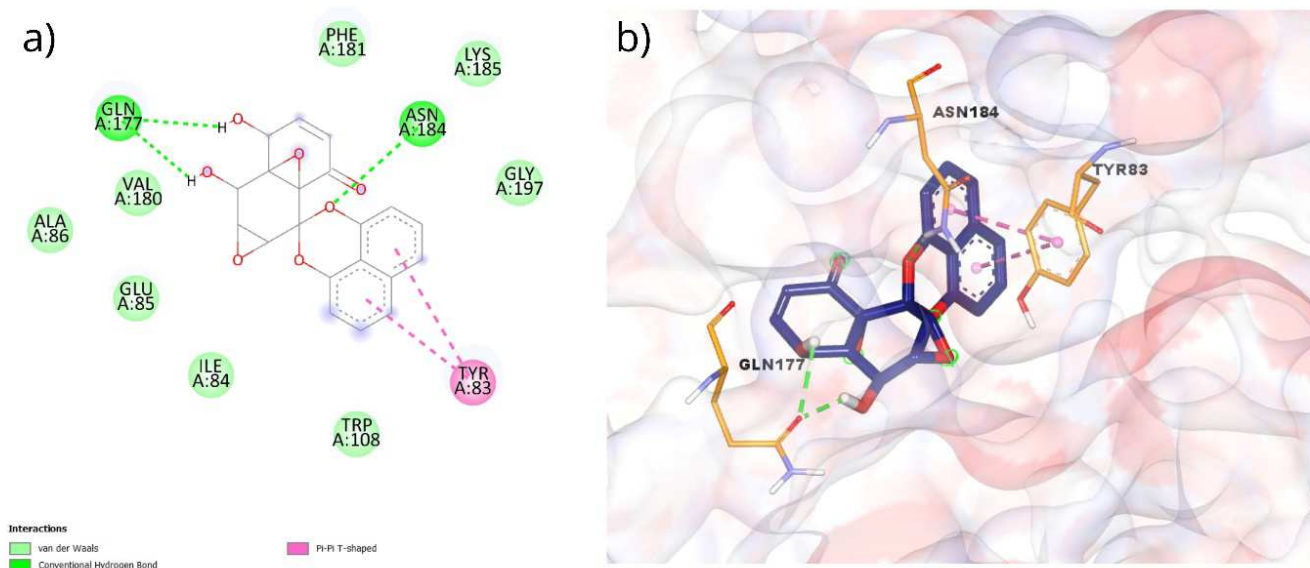


Figure 13. 2D interaction plot of Cladospirone bisepoxide docked in the binding pockets of integrase enzyme. 3D representation showing the position of Cladospirone bisepoxide within the cavity of integrase enzyme.

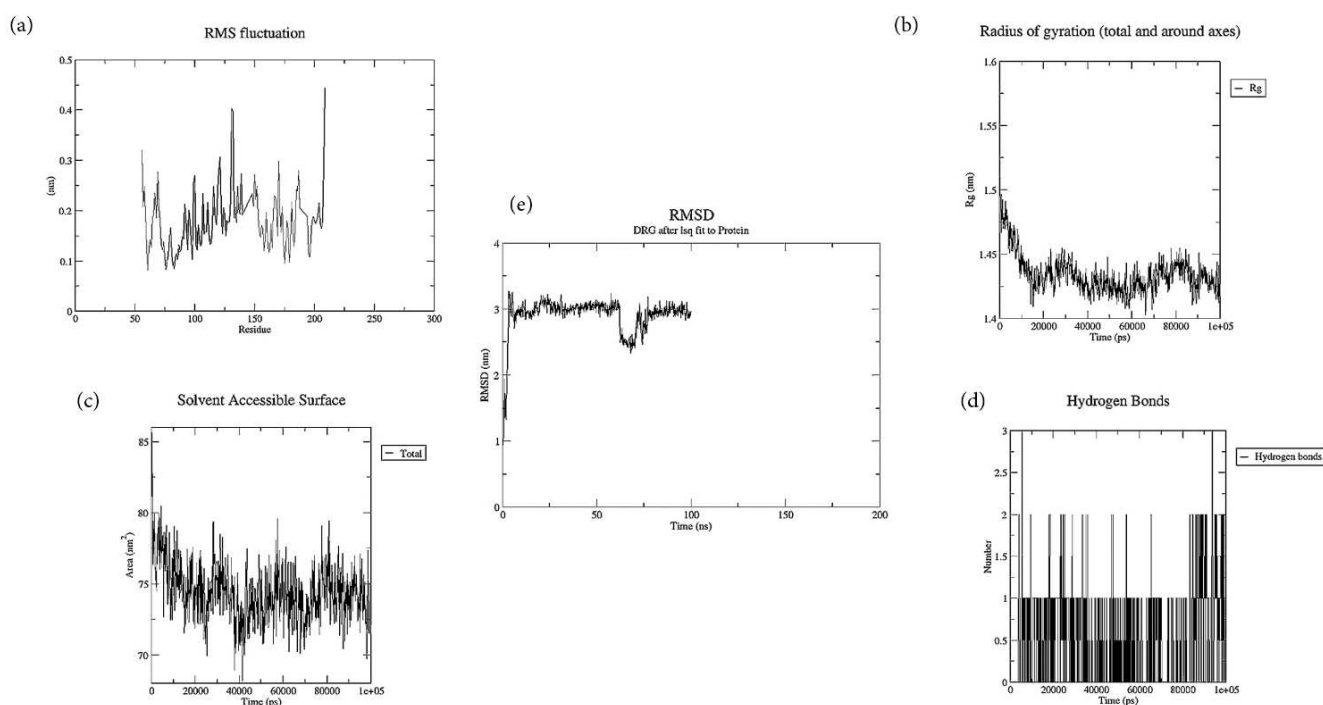


Figure 14. RMSF plot of the receptor-Cladospirone bisepoxide complex. The Radius of Gyration plot of the receptor-Cladospirone bisepoxide complex. The Solvent Accessible Surface area plot of the receptor-Cladospirone bisepoxide complex. Hydrogen bonding pattern of the receptor-Cladospirone bisepoxide complex. RMSD study plot of the receptor-Cladospirone bisepoxide complex.

The binding energy of Paulownin is -7.6 kcal/mol. It displays different types of interactions, which includes carbon hydrogen bond, pi-alkyl bond, amide pi-stacked bond, and pi-cation bond. ALA 86 of the A chain formed a carbon hydrogen bond. A chain residue VAL 180 forms pi-alkyl bond. A chain residue GLY 197 interacts with ligand by forming amide pi-stacked bond. Finally, LYS 185 of the A chain formed a pi-cation bond (Figure 15). The RMSF plot (Figure 16a) shows that the molecule has low RMSF value, indicating that structure might contain sheets and helices.

The value of the radius of gyration (Rg) shows instability of the receptor-Paulownin complex. (Figure 16b)) The solvent accessible surface area plot also shows fluctuations throughout the simulation. (Figure 16c)) Paulownin does not form hydrogen bonds with the receptor. (Figure 16d)) The RMSD plot for the receptor in complexation with Paulownin (Figure 16e)) was observed, it showed multiple fluctuations and did not attain stability throughout the simulation time. This can be attributed to the conformational changes that the receptor-Paulownin complex induce.

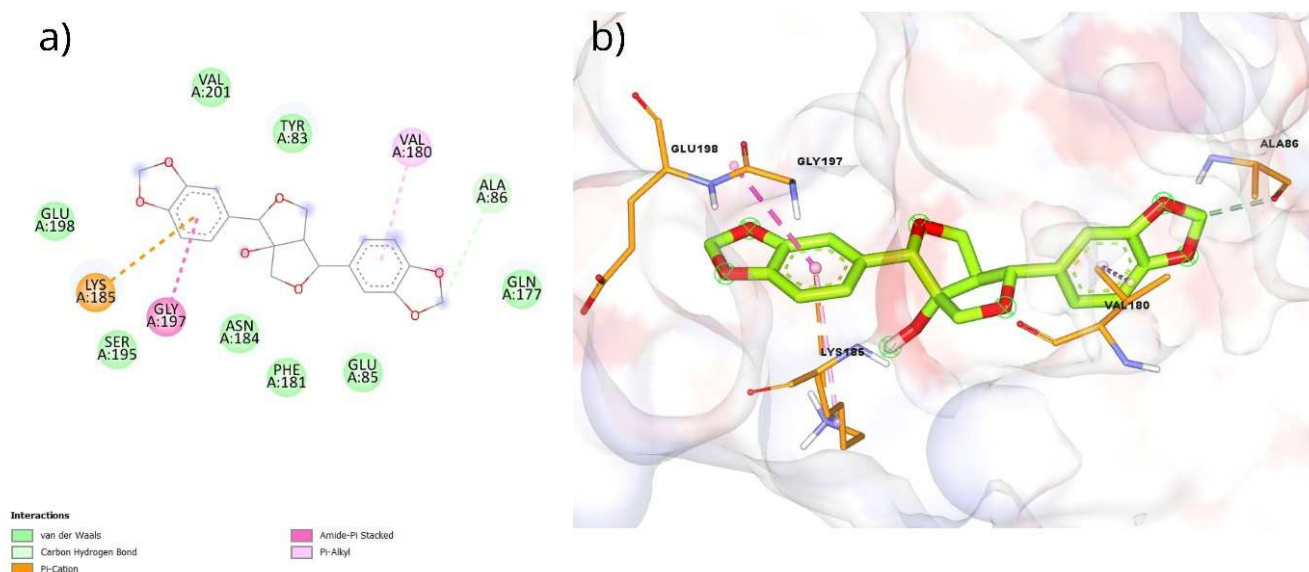


Figure 15. 2D interaction plot of Paulownin docked in the binding pockets of integrase enzyme. 3D representation showing the position of Paulownin within the cavity of integrase enzyme.

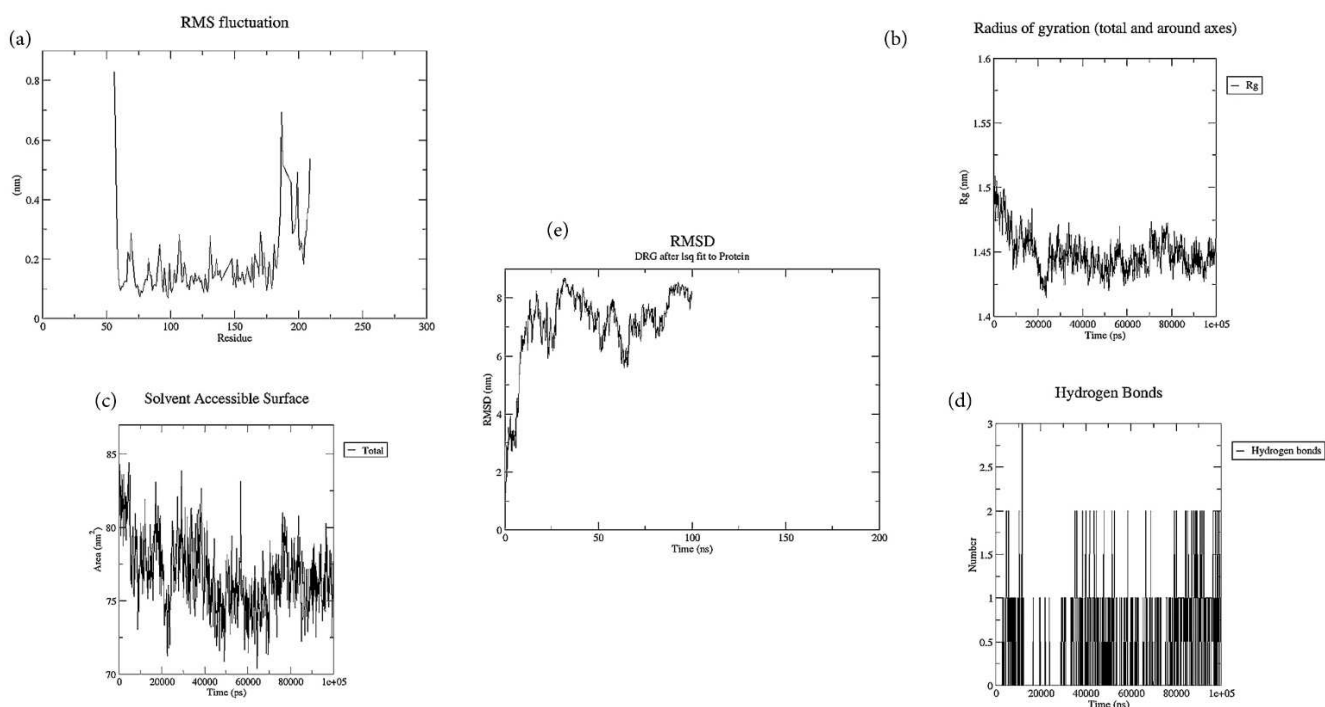


Figure 16. RMSF plot of the receptor-Paulownin complex. The Radius of Gyration plot of the receptor-Paulownin complex. The Solvent Accessible Surface area plot of the receptor-Paulownin complex. Hydrogen bonding pattern of the receptor-Paulownin complex. RMSD study plot of the receptor-Paulownin complex.

4,8-Dihydroxysesamin has a binding energy of -7.6 kcal/mol. It has five types of bonds: the conventional hydrogen bond, carbon hydrogen bond, pi-alkyl bond, alkyl bond and the pi-anion bond. TYR A-83, ASN A-184 formed the conventional hydrogen bond. GLU 87, TYR 83, PHE 181, and GLY 197 of the A chain formed carbon hydrogen bonds with the ligand. LYS 185 and VAL 180 of the A chain formed pi-alkyl and alkyl bonds, respectively. GLU A-85 forms a pi-anion bond with the target. (Figure 17) The RMSF plot (Figure 18a)) shows that the molecule

has higher RMSF values indicating that the protein has turns or loops. The radius of gyration (Rg) plot shows overall stability with some fluctuations. (Figure 18b)) The solvent accessible surface plot shows considerable fluctuations. (Figure 18c)) 4,8-Dihydroxysesamin forms two hydrogen bonds with the receptor. (Figure 18d)) In the receptor-4,8-Dihydroxysesamin complex, the RMSD values (Figure 18e)) were in the range $1.2 - 2.0$ Å with some fluctuations. The equilibration of the complex was observed between 20 to 80 ns.

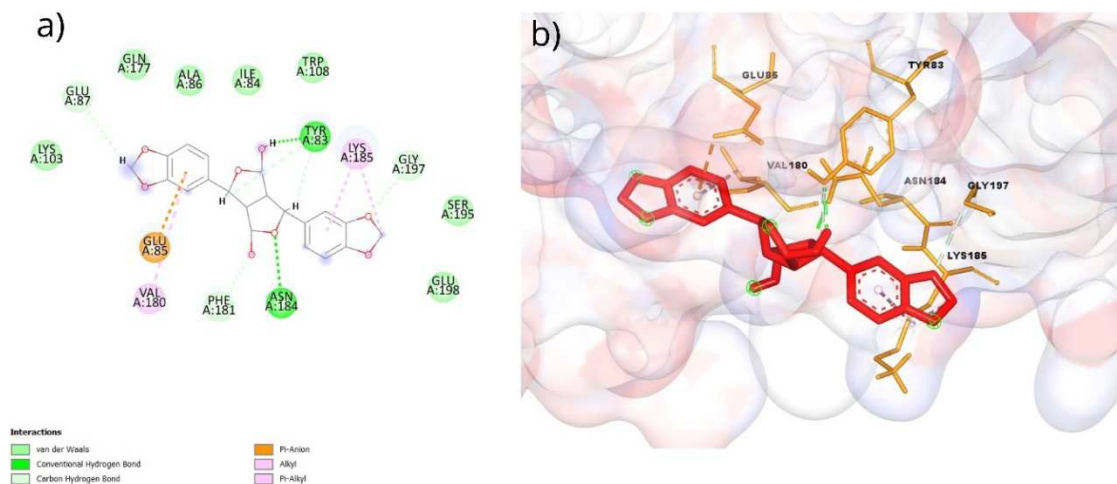


Figure 17. 2D interaction plot of 4,8-Dihydroxysesamin docked in the binding pockets of integrase enzyme. 3D representation showing the position of 4,8-Dihydroxysesamin within the cavity of integrase enzyme.

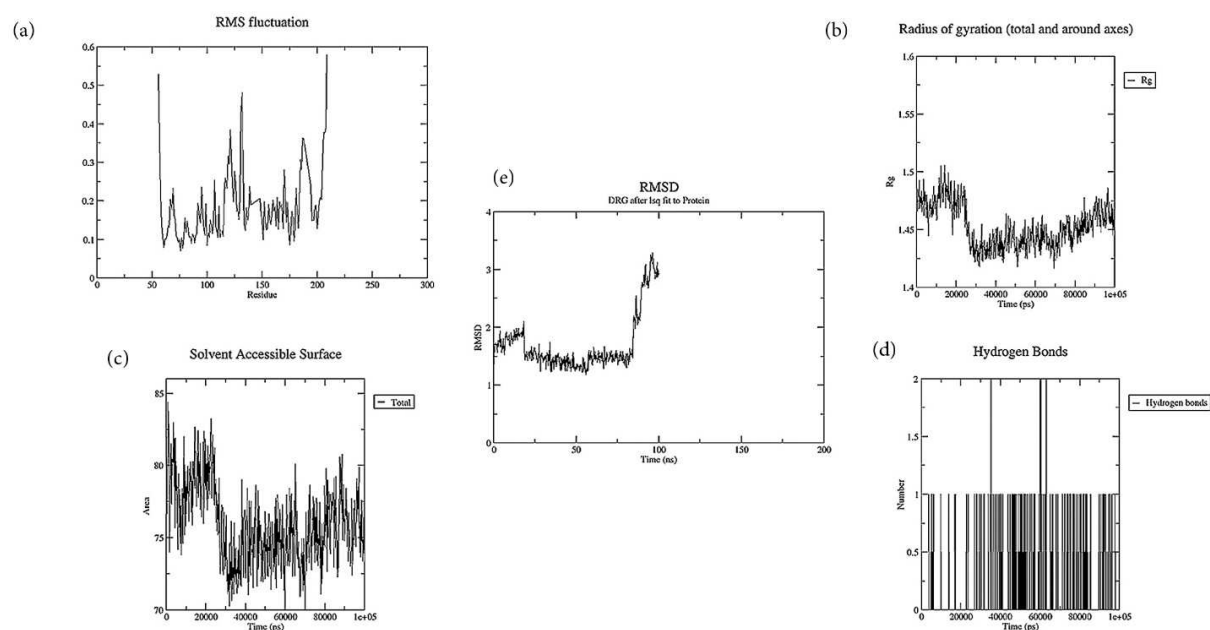


Figure 18. RMSF plot of the receptor-4,8-Dihydroxysesamin complex. The Radius of Gyration plot of the receptor-4,8-Dihydroxysesamin complex. The Solvent Accessible Surface area plot of the receptor-4,8-Dihydroxysesamin complex. Hydrogen bonding pattern of the receptor-4,8-Dihydroxysesamin complex. RMSD study plot of the receptor-4,8-Dihydroxysesamin complex.

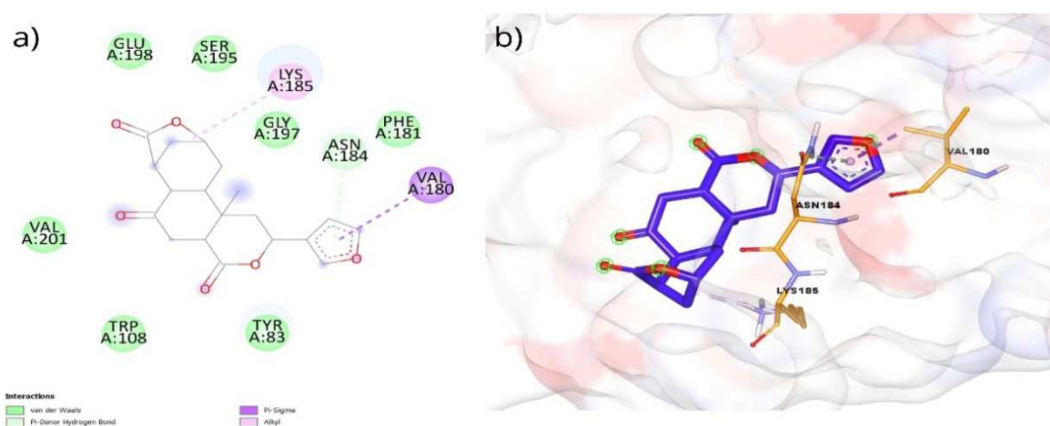


Figure 19. 2D interaction plot of Diosbulbin D docked in the binding pockets of integrase enzyme. 3D representation showing the position of Diosbulbin D within the cavity of integrase enzyme.

Diosbulbin D has a binding energy of -7.6 kcal/mol. It shows three different types of interactions: pi-donor hydrogen bond, alkyl bond, and pi-sigma bond. The A chain's ASN 184 residue forms pi-donor hydrogen bond. The residue involved in the formation of alkyl bond is LYS 185 of the chain A. VAL 180 of the A chain forms pi-sigma bond. (Figure 19) The RMSF plot (Figure 20a)) shows that Diosbulbin D has higher RMSF values. The radius of gyration (Rg) plot shows slight

fluctuations. (Figure 20b)) The solvent accessible surface area plot displays significant fluctuations. (Figure 20c)) No hydrogen bonds were formed between the receptor and Diosbulbin D. (Figure 20d)) The RMSD plot for the receptor in complexation with Diosbulbin D (Figure 20e)) was observed, it showed multiple fluctuations and did not attain stability, this can be due to the conformational changes that the receptor-Diosbulbin D complex induce.

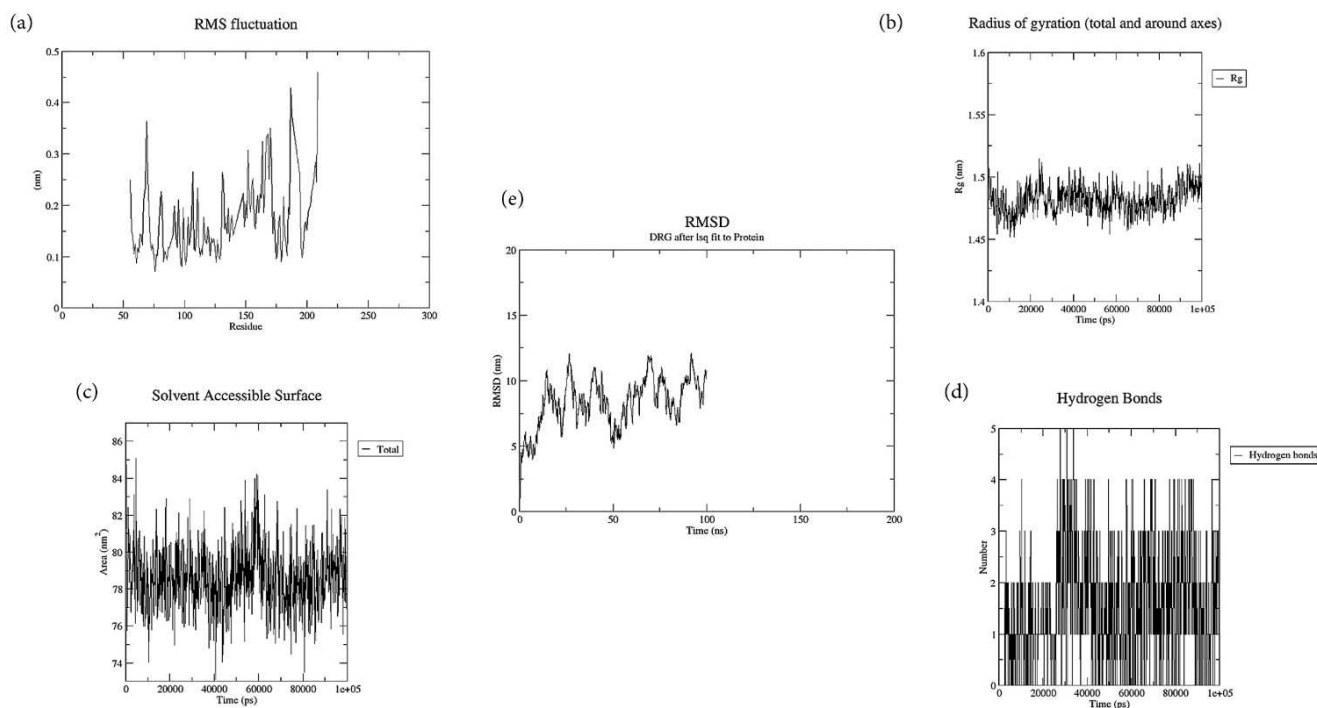


Figure 20. RMSF plot of the receptor-Diosbulbin D complex. The Radius of Gyration plot of the receptor-Diosbulbin D complex. The Solvent Accessible Surface area plot of the receptor-Diosbulbin D complex. Hydrogen bonding pattern of the receptor-Diosbulbin D complex. RMSD study plot of the receptor-Diosbulbin D complex.

4. Conclusion

Despite the availability of drugs that can be used to control the HIV infection and even reduce viral transmission, HIV remains a primary cause of death and a public health threat for millions of people throughout the world. In silico screening of bioactive molecules was carried out to identify the novel inhibitors for HIV-1 integrase enzyme. These screenings reduce the time taken to develop new drugs. The current study highlights the importance of the efficacy of in silico screening and its success in identifying HIV inhibitors that are effective against integrase enzyme.

The pharmacokinetic properties of the selected ligands were evaluated in the first round of screening, which was done using Lipinski's rule of five. This aided in the identification of the compounds, among the long list of phytochemicals, which could be further investigated. Using AutoDock technologies, computational analyses were conducted on selected phytochemicals. Molecular docking results revealed the best binding confirmation of ligands. Withaferin, Isatin, and Gummadiol had good binding

affinity while interacting with integrase enzyme. The RMSF, Radius of gyration, Hydrogen bonding pattern, and RMSD plot indicate that Isatin is the best among the seven selected ligands. The toxicity and the druggability of the ligands were further investigated in order to identify the most promising possibilities with high bioavailability and low toxicity. The toxicological prediction indicated that Isatin is safe when compared to other drugs and given in lower concentrations. As a result, in silico analysis expands the possibilities for drug development, furthermore, experimental tests must be conducted to confirm the efficiency of Isatin.

Ethics Declarations

Data Availability Statement

All data generated or analyzed during this study are included in this published article.

Author Contributions

All authors listed have made a substantial, direct, and

intellectual contribution to the work, and approved it for publication.

Conflict of Interest

All the authors do not have any possible conflicts of interest.

References

- [1] P. M. Sharp and B. H. Hahn, "Origins of HIV and the AIDS Pandemic," *Cold Spring Harb. Perspect. Med.*, vol. 1, no. 1, Sep. 2011, doi: 10.1101/CSHPERSPECT.A006841.
- [2] M. Peeters, M. Jung, and A. Ayoub, "The origin and molecular epidemiology of HIV," *Expert Rev. Anti. Infect. Ther.*, vol. 11, no. 9, pp. 885–896, Jan. 2013, doi: 10.1586/14787210.2013.825443.
- [3] F. E. McCutchan, "Global epidemiology of HIV," *J. Med. Virol.*, vol. 78, no. SUPPL. 1, Jul. 2006, doi: 10.1002/JMV.20599.
- [4] J. S. Olesen *et al.*, "HIV-2 continues to decrease, whereas HIV-1 is stabilizing in Guinea-Bissau," *AIDS*, vol. 32, no. 9, pp. 1193–1198, Jun. 2018, doi: 10.1097/QAD.0000000000001827.
- [5] Ö. Dağlı and P. T. Dergisi, "Screening of hepatitis and HIV infections in an alcohol and drug addiction treatment center," *Pamukkale Med. J.*, vol. 13, no. 1, pp. 177–186, Jan. 2020, doi: 10.31362/PATD.644886.
- [6] D. Cattaneo and C. Gervasoni, "Pharmacokinetics and Pharmacodynamics of Cabotegravir, a Long-Acting HIV Integrase Strand Transfer Inhibitor," *Eur. J. Drug Metab. Pharmacokinet.*, vol. 44, no. 3, pp. 319–327, Jun. 2019, doi: 10.1007/S13318-018-0526-2.
- [7] P. Cid-Silva *et al.*, "Clinical Experience with the Integrase Inhibitors Dolutegravir and Elvitegravir in HIV-infected Patients: Efficacy, Safety and Tolerance," *Basic Clin. Pharmacol. Toxicol.*, vol. 121, no. 5, pp. 442–446, Nov. 2017, doi: 10.1111/BCPT.12828.
- [8] A. L. Perryman *et al.*, "A Dynamic Model of HIV Integrase Inhibition and Drug Resistance," *J. Mol. Biol.*, vol. 397, no. 2, p. 600, Mar. 2010, doi: 10.1016/J.JMB.2010.01.033.
- [9] P. Gupta, P. Garg, and N. Roy, "Identification of Novel HIV-1 Integrase Inhibitors Using Shape-Based Screening, QSAR, and Docking Approach," *Chem. Biol. Drug Des.*, vol. 79, no. 5, pp. 835–849, May 2012, doi: 10.1111/J.1747-0285.2012.01326.X.
- [10] V. Dewi Prasasty, R. Anthony Hutagalung, K. Grazzolie, F. Xaverius Ivan, and C. Vivitri Dewi Prasasty, "Selective docking of promising retroviral integrase inhibitors towards prototype foamy virus integrase," ~ 265 ~ *J. Med. Plants Stud.*, vol. 6, no. 2, pp. 265–272, 2018.
- [11] A. Kolakowska, A. F. Maresca, I. J. Collins, and J. Cailhol, "Update on Adverse Effects of HIV Integrase Inhibitors," *Curr. Treat. options Infect. Dis.*, vol. 11, no. 4, pp. 372–387, Dec. 2019, doi: 10.1007/S40506-019-00203-7.
- [12] Y. Zheng *et al.*, "HPLC-MS/MS method for the simultaneous quantification of dolutegravir, elvitegravir, rilpivirine, darunavir, ritonavir, raltegravir and raltegravir-β-d-glucuronide in human plasma," *J. Pharm. Biomed. Anal.*, vol. 182, Apr. 2020, doi: 10.1016/J.JPBA.2020.113119.
- [13] P. Gupta, P. Garg, and N. Roy, "In silico screening for identification of novel HIV-1 integrase inhibitors using QSAR and docking methodologies," *Med. Chem. Res. 2013 22/10*, vol. 22, no. 10, pp. 5014–5028, Feb. 2013, doi: 10.1007/S00044-013-0490-Y.
- [14] J. Vora *et al.*, "Molecular docking, QSAR and ADMET based mining of natural compounds against prime targets of HIV," <https://doi.org/10.1080/07391102.2017.1420489>, vol. 37, no. 1, pp. 131–146, Jan. 2018, doi: 10.1080/07391102.2017.1420489.
- [15] S. K. Tripathi, C. Selvaraj, S. K. Singh, and K. K. Reddy, "Molecular docking, qpld, and adme prediction studies on hiv-1 integrase leads," *Med. Chem. Res.*, vol. 21, no. 12, pp. 4239–4251, Dec. 2012, doi: 10.1007/S00044-011-9940-6.
- [16] R. Singh, A. Nath, and B. Sharma, "Docking Studies of HIV-1 Reverse Transcriptase and HIV-1 Integrase with Phytocompounds of Carissa Carandas L.," *J. Clin. Res. HIV AIDS Prev.*, vol. 3, no. 4, pp. 10–19, May 2019, doi: 10.14302/ISSN.2324-7339.JCRHAP-19-2847.
- [17] V. Jha *et al.*, "Human immunodeficiency virus type 1: Role of proteins in the context of viral life cycle," *J Adv Biotechnol Exp Ther.*, vol. 5, no. 2, pp. 307–319, 2022, doi: 10.5455/jabet.2022.d117.
- [18] S. K. Burley *et al.*, "RCSB Protein Data Bank: Powerful new tools for exploring 3D structures of biological macromolecules for basic and applied research and education in fundamental biology, biomedicine, biotechnology, bioengineering and energy sciences," *Nucleic Acids Res.*, vol. 49, no. 1, pp. D437–D451, 2021, doi: 10.1093/NAR/GKAA1038.
- [19] J. A. Duke, "Database of Biologically Active Phytochemicals & Their Activity," *Boca Raton, Fla CRC Press.*, p. 183, 1992.
- [20] K. Mohanraj *et al.*, "IMPPAT: A curated database of Indian Medicinal Plants, Phytochemistry And Therapeutics OPEN," *Sci. REPoRTS*], vol. 8, p. 4329, 2018, doi: 10.1038/s41598-018-22631-z.
- [21] S. Kim *et al.*, "PubChem in 2021: New data content and improved web interfaces," *Nucleic Acids Res.*, vol. 49, no. D1, pp. D1388–D1395, Jan. 2021, doi: 10.1093/nar/gkaa971.
- [22] A. Daina, O. Michielin, and V. Zoete, "SwissADME: a free web tool to evaluate pharmacokinetics, drug-likeness and medicinal chemistry friendliness of small molecules," *Sci. Reports 2017 71*, vol. 7, no. 1, pp. 1–13, Mar. 2017, doi: 10.1038/srep42717.
- [23] L. Z. Benet, C. M. Hosey, O. Ursu, and T. I. Oprea, "BDDCS, the Rule of 5 and Drugability Graphical abstract HHS Public Access," *Adv Drug Deliv Rev.*, vol. 101, pp. 89–98, 2016, doi: 10.1016/j.addr.2016.05.007.
- [24] E. F. Pettersen *et al.*, "UCSF Chimera--a visualization system for exploratory research and analysis," *J. Comput. Chem.*, vol. 25, no. 13, pp. 1605–1612, Oct. 2004, doi: 10.1002/JCC.20084.

- [25] S. Dallakyan and A. J. Olson, "Small-molecule library screening by docking with PyRx," *Methods Mol. Biol.*, vol. 1263, pp. 243–250, 2015, doi: 10.1007/978-1-4939-2269-7_19.
- [26] V. Jha *et al.*, "Screening of Phytochemicals as Potential Inhibitors of Breast Cancer using Structure Based Multitargeted Molecular Docking Analysis," *Phytomedicine Plus*, vol. 2, no. 2, May 2022, doi: 10.1016/j.phyplu.2022.100227.
- [27] E. Bursal *et al.*, "Determination of Phenolic Content, Biological Activity, and Enzyme Inhibitory Properties with Molecular Docking Studies of *Rumex nepalensis*, an Endemic Medicinal Plant," *J. Food Nutr. Res.*, vol. 9, no. 3, pp. 114–123, Mar. 2021, doi: 10.12691/JFNR-9-3-3.
- [28] Lindahl, Abraham, Hess, and van der Spoel, "GROMACS 2021 Source code," Jan. 2021, doi: 10.5281/ZENODO.4457626.
- [29] P. Banerjee, A. O. Eckert, A. K. Schrey, and R. Preissner, "ProTox-II: a webserver for the prediction of toxicity of chemicals," *Nucleic Acids Res.*, vol. 46, pp. 257–263, 2018, doi: 10.1093/nar/gky318.
- [30] G. Xiong *et al.*, "ADMETlab 2.0: an integrated online platform for accurate and comprehensive predictions of ADMET properties," *Nucleic Acids Res.*, vol. 49, no. W1, pp. W5–W14, Jul. 2021, doi: 10.1093/NAR/GKAB255.
- [31] R. Akbar and W. K. Yam, "Interaction of ganoderic acid on HIV related target: molecular docking studies," *Bioinformation*, vol. 7, no. 8, pp. 413–417, Dec. 2011, doi: 10.6026/97320630007413.
- [32] R. G. Maroun *et al.*, "Self-association and Domains of Interactions of an Amphipathic Helix Peptide Inhibitor of HIV-1 Integrase Assessed by Analytical Ultracentrifugation and NMR Experiments in Trifluoroethanol/H₂O Mixtures *," *J. Biol. Chem.*, vol. 274, no. 48, pp. 34174–34185, Nov. 1999, doi: 10.1074/JBC.274.48.34174.
- [33] C. A. Lipinski, F. Lombardo, B. W. Dominy, and P. J. Feeney, "Experimental and computational approaches to estimate solubility and permeability in drug discovery and development settings," *Adv. Drug Deliv. Rev.*, vol. 46, no. 1–3, pp. 3–26, Mar. 2001, doi: 10.1016/S0169-409X(00)00129-0.
- [34] D. F. Veber, S. R. Johnson, H. Y. Cheng, B. R. Smith, K. W. Ward, and K. D. Kopple, "Molecular properties that influence the oral bioavailability of drug candidates," *J. Med. Chem.*, vol. 45, no. 12, pp. 2615–2623, Jun. 2002, doi: 10.1021/JM020017N.
- [35] D. Dahlgren, M. Sjöblom, and H. Lennernäs, "Intestinal absorption-modifying excipients: A current update on preclinical in vivo evaluations," *Eur. J. Pharm. Biopharm.*, vol. 142, pp. 411–420, Sep. 2019, doi: 10.1016/J.EJPB.2019.07.013.
- [36] P. Tripathi, S. Ghosh, and S. Nath Talapatra, "Bioavailability prediction of phytochemicals present in *Calotropis procera* (Aiton) R. Br. by using Swiss-ADME tool," *World Sci. News*, vol. 131, pp. 147–163, 2019, Accessed: Jun. 17, 2022. [Online]. Available: www.worldscientificnews.com
- [37] Y. S. Krishnaiah, "Pharmaceutical Technologies for Enhancing Oral Bioavailability of Poorly Soluble Drugs," *J Bioequiv Availab*, vol. 2, no. 2, pp. 28–36, 2010, doi: 10.4172/jbb.1000027.
- [38] P. Baghel, A. Roy, S. Verma, T. Satapathy, and S. Bahadur, "Amelioration of lipophilic compounds in regards to bioavailability as self-emulsifying drug delivery system (SEDDS)," *Futur. J. Pharm. Sci.* 2020 61, vol. 6, no. 1, pp. 1–11, Jun. 2020, doi: 10.1186/S43094-020-00042-0.
- [39] V. Jha *et al.*, "Computational screening of phytochemicals to discover potent inhibitors against chikungunya virus," *Vegetos*, vol. 34, no. 3, pp. 515–527, Sep. 2021, doi: 10.1007/S42535-021-00227-9.
- [40] M. J. Waring, "Lipophilicity in drug discovery," *Expert Opin. Drug Discov.*, vol. 5, no. 3, pp. 235–248, Mar. 2010, doi: 10.1517/17460441003605098.
- [41] M. D. Segall and C. Barber, "Addressing toxicity risk when designing and selecting compounds in early drug discovery," *Drug Discov. Today*, vol. 19, no. 5, pp. 688–693, 2014, doi: 10.1016/J.DRUDIS.2014.01.006.
- [42] D. B. Kitchen, H. Decornez, J. R. Furr, and J. Bajorath, "Docking and scoring in virtual screening for drug discovery: methods and applications," *Nat. Rev. Drug Discov.*, vol. 3, no. 11, pp. 935–949, Nov. 2004, doi: 10.1038/NRD1549.
- [43] L. Pinzi and G. Rastelli, "Molecular Docking: Shifting Paradigms in Drug Discovery," *Int. J. Mol. Sci.*, vol. 20, no. 18, Sep. 2019, doi: 10.3390/IJMS20184331.
- [44] L. Martínez, "Automatic identification of mobile and rigid substructures in molecular dynamics simulations and fractional structural fluctuation analysis," *PLoS One*, vol. 10, no. 3, Mar. 2015, doi: 10.1371/JOURNAL.PONE.0119264.